Articles

Recognition-Mediated Assembly of Nanoparticle-Diblock Copolymer Micelles with Controlled Size

Oktay Uzun, Benjamin L. Frankamp, Amitav Sanyal, and Vincent M. Rotello*

Department of Chemistry, University of Massachusetts, Amherst, Massachusetts 01003

Received June 28, 2006. Revised Manuscript Received September 7, 2006

Random polystyrene-based diblock copolymers with strongly interacting hydrogen-bonding units, diaminotriazine (triaz) functionality, on one of the blocks (PS/S-triaz) were used to assemble complementary thymine (Thy)-functionalized gold nanoparticles (Thy−Au) into micellar aggregates. The role of each of these blocks on the aggregate size was investigated by synthesizing two different series of diblock copolymers: in the first series unfunctionalized block (polystyrene block) length was kept constant and the recognition element functionalized block (triaz block) length increased; in the second series, triaz block length was kept constant and polystyrene block length increased. The size of these self-assembled aggregates was determined in solution by using dynamic light scattering and in thin films by using transmission electron microscopy and small-angle X-ray scattering.

Introduction

Increased device performance has been recognized through the steady miniaturization in the feature sizes of transistors in electronic circuits.[1] Traditional "top-down" lithographic fabrication techniques are expected to reach their physical limits in their ability to produce sub-40-nm features.[2] "Bottom-up" fabrication methods based on self-assembly of complementary functionalities offer a new approach for the successful fabrication of next-generation devices. Bottom-up directed assembly has features that offer the promise of nanostructured fabrication of devices for applications such as sensing,[3] integration with biotechnology,[4] and quantum computers.[5]

Metal and semiconductor nanoparticles embedded in polymer matrixes provide materials that possess the unique properties arising from the nanoscopic size and shapes of the metal clusters.[6] The ability to use nanoparticle properties for device fabrication will require the formation of highly ordered arrays of nanoparticles.[7] Self-assembly of nanoparticles mediated by polymers presents a powerful bottom-up approach to construct stabilized metal and semiconductor nanocomposites as well as allows for the fabrication of new structured nanoscale materials.[8] Several attributes of the individual building blocks such as the size and shape of individual metal clusters, composition of the monolayer, and functional groups on the polymers allow control over the

* To whom correspondence should be addressed. Tel: (413) 545-2058. Fax: (413) 545-4490. E-mail: rotello@chem.umass.edu.

(1) Lundstrom, M. *Science* **2003,** *299,* 210−211.
(2) Wallraff, G. M.; Hinsberg, W. D. *Chem. Rev.* **1999**, *99,* 1801.
(3) Zayats, M.; Pogorelova, S. P.; Kharitonov, A. B.; Lioubashevski, O.; Katz, E.; Willner, I. *Chem-Eur J.* **2003,** *9,* 6108−6114. Shipway, A. N.; Katz, E.; Willner, I. *ChemPhysChem.* **2000,** *1,* 18−52.
(4) (a) Katz, E.; Willner, I. *Angew. Chem., Int. Ed.* **2004,** *43,* 6042−6108. (b) Xiao, Y.; Patolsky, F.; Katz, E.; Hainfeld, J. F.; Willner, I. *Science* **2003,** *299,* 1877−1881. (c) Csaki, A.; Maubach, G.; Born, D.; Reichert, J.; Fritzsche, W. *Single Mol.* **2002,** *3,* 275−280. Patolsky, F.; Weizmann, Y.; Willner, I. *Nat. Mater.* **2004,** *3,* 692−695.
(5) (a) McEuen, P. L. *Science* **1997**, *278,* 1729. (b) Lloyd, S. *Science* **1993**, *261,* 1569.
(6) (a) Daniel, M. C.; Astruc, D. *Chem. Rev.* **2004,** *104,* 293−346. (b) Love, J. C.; Estroff, L. A.; Kriebel, J. K.; Nuzzo, R. G.; Whitesides, G. M. *Chem. Rev.* **2005,** *105,* 1103−1169. (c) Rana, R. K.; Murthy, V. S.; Yu, J.; Wong, M. S. *Adv. Mater.* **2005,** *17,* 1145−1150. (d) Corbierre, M. K.; Cameron, N. S.; Sutton, M.; Laaziri, K.; Lennox, R. B. *Langmuir* **2005,** *21,* 6063−6072. (e) Patton, D.; Locklin, J.; Meredith, M.; Xin, Y.; Advincula, R. *Chem. Mater.* **2004,** *16,* 5063−5070. (f) Park, J. H.; Lim, Y. T.; Park, O. O.; Kim, J. K.; Yu, J. W.; Kim, Y. C. *Chem. Mater.* **2004,** *16,* 688−692. (g) Tian, S. J.; Liu, J. Y.; Zhu, T.; Knoll, W. *Chem. Mater.* **2004,** *16,* 4103−4108.
(7) (a) Sun, S.; Anders, S.; Hamann, H. F.; Thiele, J.-U.; Baglin, J. E. E.; Thomson, T.; Fullerton, E. E.; Murray, C. B.; Terris, B. D. *J. Am. Chem. Soc.* **2002**, *124,* 2884. (b) Sun, S.; Anders, S.; Thomson, T.; Baglin, J. E. E.; Toney, M. F.; Hamann, H. F.; Murray, C. B.; Terris, B. D. *J. Phys. Chem. B* **2003**, *107,* 5419. (c) Bockstaller, M. R.; Thomas, E. L. *J. Phys. Chem. B* **2003,** *107,* 10017−10024. (d) Sun, S. H.; Murray, C. B.; Weller, D.; Folks, L.; Moser, A. *Science* **2000**, *287,* 1989−1992. (e) Kiely, C. J.; Fink, J.; Brust, M.; Bethell, D.; Schiffrin, D. J. *Nature* **1998**, *396,* 444−446. (f) Kim, B.; Trip, S. L.; Wei, A. *J. Am. Chem. Soc.* **2001**, *123,* 7955−7956. (g) Marinakos, S. M.; Shultz, D. A.; Feldheim, D. L. *Adv. Mater.* **1999**, *11,* 34−37. (h) Novak, J. P.; Feldheim, D. L. *J. Am. Chem. Soc.* **2000**, *122,* 3979−3980. (i) Jin, J.; Iyoda, T.; Cao, C. S.; Song, Y. L.; Jiang, L.; Li, T. J.; Ben Zhu, D. *Angew. Chem., Int. Ed.* **2001**, *40,* 2135−2138. (j) Liu, J.; Mendoza, S.; Roman, E.; Lynn, M. J.; Xu, R. L.; Kaifer, A. E. *J. Am. Chem. Soc.* **1999**, *121,* 4304−4305. (k) Schmid, G.; Chi, L. F. *Adv. Mater.* **1998**, *10,* 515−526.
(8) (a) Shenhar, R.; Norsten, T. B.; Rotello, V. M. *Adv. Mater.* **2005,** *17,* 657−669. (b) Kang, Y. J.; Taton, T. A. *Macromolecules* **2005,** *38,* 6115−6121. (c) Glass, R.; Moller, M.; Spatz, J. P. *Nanotechnology* **2003,** *14,* 1153−1160. (d) Lopes, W. A.; Jaeger, H. M. *Nature* **2001,** *414,* 735−738. (e) Mossmer, S.; Spatz, J. P. *Angew. Chem., Int. Ed.* **2002,** *114,* 3359. (f) Mayer, A. B. R. *Polym. Adv. Technol.* **2001**, *12,* 96−106. (g) Sohn, B. H.; Seo, B. H. *Chem. Mater.* **2001**, *13,* 1752−1757. (h) Watson, K. J.; Park, S. J.; Im, J. H.; Nguyen, S. T.; Mirkin, C. A. *J. Am. Chem. Soc.* **2001**, *123,* 5592−5593. (i) Zehner, R.W.; Lopes, W. A.; Morkved, T. L.; Jaeger, H.; Sita, L. R. *Langmuir* **1998**, *14,* 241−244.

10.1021/cm0614968 CCC: $33.50
Published on Web 10/21/2006

properties of these constructs. Additional control over the structure and morphology of such nanocomposites can be induced by the modifications in the polymer structure. Such fabrication of composite materials using the assembly of nanoscopic building blocks or the bottom-up approach provides a methodology complementary to top-down lithographic methods. The bottom-up approach provides access to smaller structures with better three-dimensional control than sophisticated lithographic techniques such as electron-beam lithography.[9] Such multiscale engineering would allow fabrication of complex functional devices with atomic level structural control.

In recent research, we developed a polymer-mediated "bricks and mortar" strategy affording unique capabilities for the bottom-up assembly of nanoparticles into macroscopic objects.[10] In this investigation, 2 nm gold nanoparticles featuring thymine functionality were assembled into spherical aggregates using a monoblock triaz-functionalized polymer through specific three-point hydrogen-bonding interactions (Figure 1). The control experiment with the *N*-methylthymine−gold nanoparticle showed no aggregation after polymer addition; this confirms that self-assembly did not take place and that specific three-point hydrogen bonding is necessary for aggregate formation. With variation of the temperature during the assembly process, aggregates ranging from 100 to 1000 nm in diameter could be formed. The key limitation of this method, however, is that aggregate size and shape that were controlled by the complex thermodynamics of the self-assembly process prevented access to structures smaller than 100 nm and made formation of larger particles a trial-and-error process. To overcome the limitations of the size and structure of these aggregates, a series of diblock copolymers were prepared for the nanoparticle assembly. The initial part of the polystyrene backbone was left unfunctionalized to prevent extensive aggregation and the second part was functionalized with the triaz recognition group; in other words, the utility of recognition element-functionalized diblock copolymers was investigated as a mortar for the assembly of nanoparticle bricks. Microscopy of the resultant thin films confirmed the self-assembly process and the formation of spherical micellar aggregates smaller than 100 nm. This new synthetic approach for nanoparticle assembly utilizes the advantage of micro phase separation of the copolymer to provide control of aggregate size through changes in block length of the diblock copolymer.[11] This method can be easily applied to the size-controlled formation of nanoparticle aggregates in solution and in thin films. However, diblock copolymers used in this study were composed of symmetrical block lengths (both blocks changed by the same amount); these series of polymers prevented us from probing the individual chain length effects on the aggregate size and morphology. To expand the range of sizes available using this assembly method and to investigate the role of each block independent of the other, a larger series of polymers were required to be analyzed. Herein, we report our recent investigations on the role of each of these blocks on the aggregate size by synthesizing two different series of diblock copolymers: In the first series unfunctionalized block (polystyrene block) length was kept constant and the recognition element functionalized block (triaz block) length increased; this series thus allowed the investigation of the influence of unfunctionalized polystyrene chain length on the aggregate size. In the second series, the triaz block length was kept constant and polystyrene block length increased; this series therefore allowed quantitative probing of the contribution of varying polymer lengths on the aggregate size of the assemblies. The size of these self-assembled aggregates was determined in solution by using dynamic light scattering (DLS) and in thin films by using transmission electron microscopy (TEM).

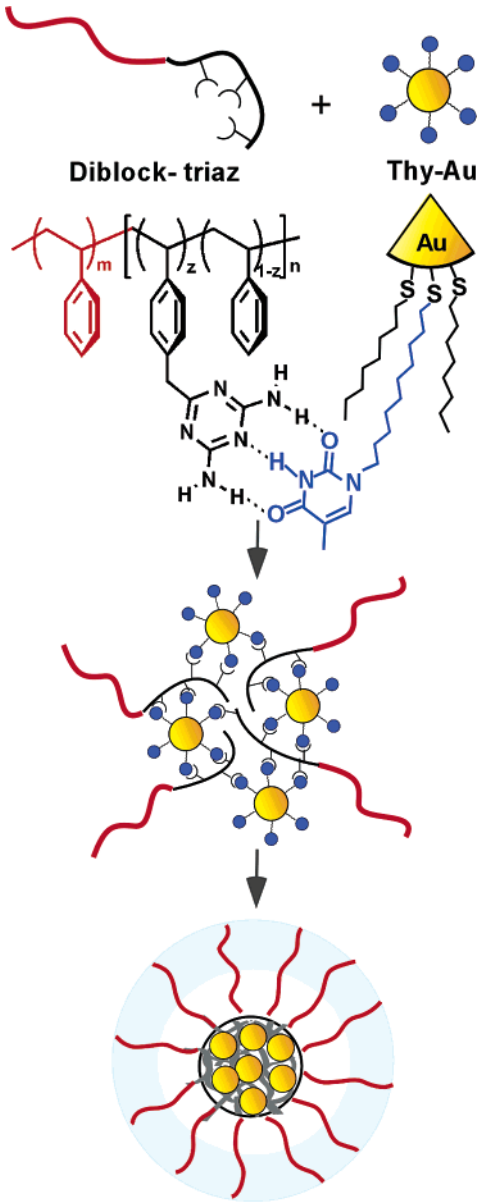

Figure 1. Schematic illustration of micelle formation with thymine-functionalized gold nanoparticle (Thy−Au) and diaminotriazine-functionalized diblock copolymer (PS/S-triaz).

(9) (a) Jager, E. W. H.; Smela, E.; Inganas, O. *Science* **2000**, *290*, 1540. (b) Chen, Y.; Pepin, A. *Electrophoresis* **2001**, *22*, 187. (c) Craighead, H. G. *Science* **2000**, *290*, 1532. (d) Wallraff, G. M.; Hinsberg, W. D. *Chem. Rev.* **1999**, *99*, 1801.

(10) Boal, A. K.; Ilhan, F.; DeRouchey, J. E.; Thurn-Albrecht, T.; Russell, T. P.; Rotello, V. M., *Nature* **2000,** *404*, 746−748.

(11) Frankamp, B. L.; Uzun, O.; Ilhan, F.; Boal, A. K.; Rotello, V. M. *J. Am. Chem. Soc.* **2002,** *124*, 892−893.

Table 1. Molecular Attributes of Parent PS/S-CMS Polymers

notation	M_n (kg/mol)[a] PS[b]	P(S-CMS)	total	PDI[a]	DP[a,c,d]	functionality content[a,d,e] (mol %)
PS/S-CMS (13:13)	12.7	13.1	25.8	1.16	239	17%
PS/S-CMS (20:13)	20.6	13.7	34.5	1.20	290	19%
PS/S-CMS (27:13)	27.1	12.7	39.8	1.26	370	17%
PS/S-CMS (27:20)	27.1	20.1	47.2	1.23	434	23%
PS/S-CMS (27:26)	27.1	26.2	53.3	1.25	489	22%
PS/S-CMS (20:20)	20.9	18.7	39.6	1.16	370	16%

[a] According to SEC with PS standards. [b] PDI of all PS blocks were ca. 1.1. [c] Average total degree of polymerization. [d] Calculated from ^{1}H NMR integration. [e] Molar percentage of CMS (in the case of block copolymers it represents the percentage within the functionalized block only).

Results and Discussion

Synthesis of Diblock Copolymers. The diblock copolymers required for the assembly process were synthesized using the nitroxide-mediated radical polymerization,[12] with the first block polystyrene and the second block a random copolymer of styrene and chloromethylstyrene (CMS). Incorporation ratios of the CMS units into the random copolymer block were determined to be 16−23% by NMR integration values. These polymers were then converted into the (PS/S-triaz) polymers through reaction with sodium cyanide followed by dicyandiimide.[13]

Thy−Au (thymine-functionalized gold) nanoparticles were made via place displacement[14] of a thymine-functionalized thiol into octanethiol-protected gold nanoparticle prepared using the Brust-Schiffrin method.[15]

The diblock copolymers used in this study (see Table 1) are meant to probe the role of each of these blocks on the aggregate size and morphology. The first series is comprised of three polymers with characteristics of PS/S-triaz (13:13), PS/S-triaz (20:13), and PS/S-triaz (27:13) in which the molecular weights in the recognition element functionalized block (triaz block) length were kept constant and polystyrene block length was increased with similar functionality content. This series thus allows the investigation of the influence of unfunctionalized polystyrene chain length on the aggregate size.

The second one consists of three polymers having characteristics of PS/S-CMS (27:13), PS/S-CMS (27:20), and PS/S-CMS (27:26), with the polystyrene block length kept constant at 27000 and the triaz block length increased from 13000 to 27000 in which the functionality content is very similar. This series therefore allows quantitative probing of the contribution of varying polymer lengths (derived from changes in the functionalized block lengths) on the aggregate size of the assemblies. Polymers synthesized with a larger functionalized block than unfunctionalized were not soluble and were not investigated.

Table 2. Size Data for Copolymer Thy−Au Aggregates with Diblock Copolymers

notation	R_h[a] (nm)	core radii[b] (nm)
PS/S-triaz (13:13)	18.8	17.4
PS/S-triaz (20:13)	18.2	14.6
PS/S-triaz (27:13)	19.1	13.5
PS/S-triaz (27:20)	24.8	17.1
PS/S-triaz (27:26)	31.3	29.0
PS/S-triaz (20:20)	20.2	14.8

[a] DLS, standard deviation obtained from size distribution diagram ± 6 nm. [b] Determined from TEM images of aggregate core, standard deviation ± 1.8 nm obtained from ∼100 aggregates/sample.

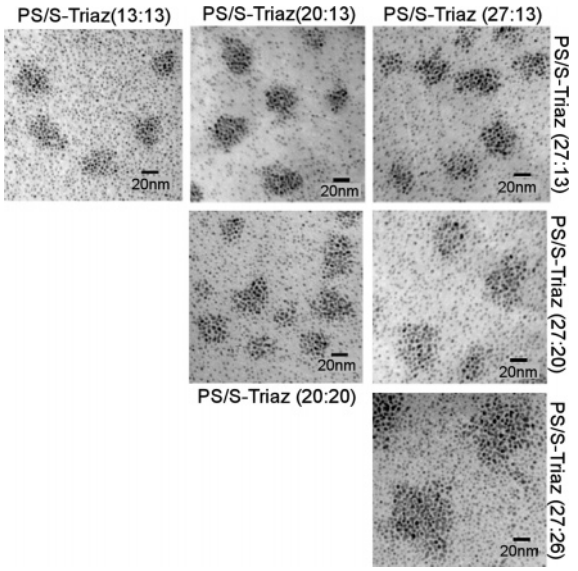

Figure 2. Spherical micellar structures formed by assembly of Thy−Au by polymers (a) PS/S-triaz (13:13), PS/S-triaz (20:13), PS/S-triaz (27:13), (b) PS/S-triaz (27:13), PS/S-triaz (27:20), and PS/S-triaz (27:26); these micrographs clearly show incorporation of Thy−Au into the micelle.

Characterization of Diblock Assemblies. Aggregation in solution was demonstrated using dynamic light acattering (DLS) on dilute solutions of Au−Thy solutions with 0.25 mg/mL and polymer solutions of 0.5 mg/mL in $CHCl_3$. As hypothesized, the size of these aggregates increased with the size of the polymer by the increase in hydrodynamic radius (R_h) from 18.8 to 31.3 nm (Table 2).

Transmission electron microscopy (TEM) provided further insight into the structure of the aggregates. Solutions of diblock copolymers (0.5 mg/mL) and Thy-capped−Au (2 mg/mL) nanoparticles allowed for brief incubation and were drop cast on to a TEM grid. TEM not only allowed the confirmation of micellar shape but also provided an efficient way to analyze aggregate core size. Concurrent with the trend observed between the polymer molecular weight and the solution hydrodynamic radius, the aggregate core sizes enlarged with increasing polymer length (Figure 2).

Further examination of the micrographs revealed that both core size and structure are dependent on individual polymer block lengths. There were two evident trends from these assemblies: by keeping the triaz-functionalized block length constant at 13000 and changing the unfunctionalized block from 13000, 20000, to 27000. As the size of the unfunctionalized block increased, we observed a decrease in the

(12) (a) Hawker, C. J.; Bosman, A. W.; Harth, E. *Chem. Rev.* **2001**, *101*, 3661−3688. (b) Harth, E.; Hawker, C. J.; Fan, W.; Waymouth, R. M. *Macromolecules* **2001**, *34*, 3856−3862. (c) Benoit, D.; Chaplinski, V.; Braslau, R.; Hawker, C. J. *J. Am. Chem. Soc.* **1999**, *121*, 3904−3920.
(13) Ilhan, F.; Gray, M.; Rotello, V. M. *Macromolecules* **2001**, *34*, 2597−2601.
(14) Ingram, R. S.; Hostetler, M. J.; Murray, R. W. *J. Am. Chem. Soc.* **1997**, *119*, 9175−9178.
(15) (a) Brust, M.; Walker, M.; Bethell, D.; Schiffrin, D. J.; Whyman, R. *Chem. Commun*. **1994**, 801−802. (b) Zamborini, F. P.; Gross, S. M.; Murray, R. W. *Langmuir* **2001**, *17*, 481−488. (c) Teranishi, T.; Hasegawa, S.; Shimizu, T.; Miyake, M. *Adv. Mater.* **2001,** *13*, 1699−1701.

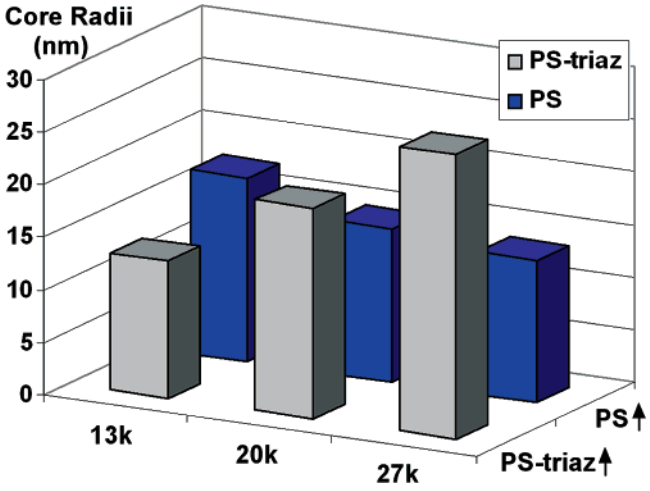

Figure 3. Graph of change in core radii for Thy−Au aggregates with diblock copolymer block length: (a) PS block increased and PS-triaz kept constant (blue); (b) PS-triaz block length increased and PS block kept constant (gray).

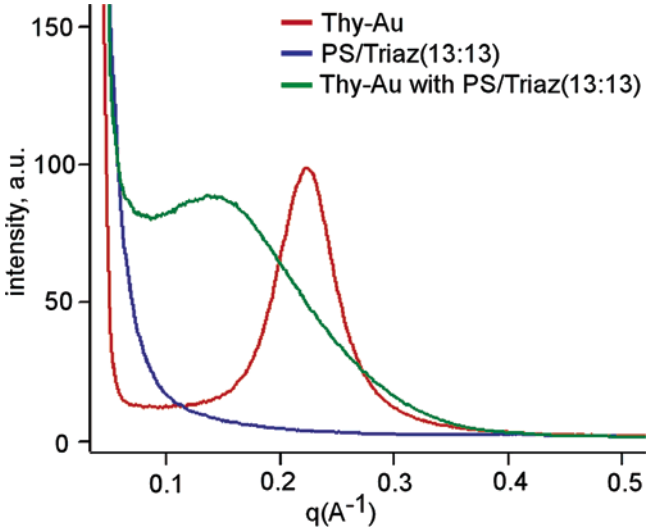

Figure 4. SAXS curves of structures formed by assembly of Thy−Au with PS/S-triaz (13:13) block copolymer. (a) Thy−Au nanoparticles drop cast from chloroform, red curve; (b) diblock copolymer PS/S-triaz (13:13), blue curve; (c) assembly of Thy−Au with PS/S-triaz (13:13) block copolymer, green curve.

core size of the spherical aggregates (Figure 3, blue bar). This change in size is expected; increasing the length of the unfunctionalized polystyrene block increases the curvature of the micelle, with concomitant decrease in core diameter.

In the second series the unfunctionalized block was held constant, while the triaz block was increased in size. In this case aggregate core size was bigger as the block length of triaz was increased, indicating that the increased block length allows more nanoparticles to be incorporated into the core of the micelle (Figure 3, gray bar). This series also gave more insight into the degree of stretching of the triaz block in the cores; concurrent with the trend observed between the polymer length and the overall diameter determined from DLS, the core radii were more than 70% of the combined core and corona, indicating that the polymer chains within the core are somewhat extended relative to the polystyrene corona.

Small-angle X-ray scattering (SAXS) at wide scattering angles were used to analyze the structural characteristics of PS/S-triaz (13:13) block copolymer/Thy−Au nanoparticle assemblies.[16] Thy−Au nanoparticles drop cast from chloroform have a scattering vector (q) with maximum intensity at 0.22423 A^{-1}. This q value can be converted to distance through the relationship ($q = 2\pi/d$) with the resultant center-to-center particle spacing of 2.8 nm (Figure 4). This result is concurrent with particles spaced only by their monolayer. When PS/S-triaz(13:13) block copolymer was used to assemble Thy−Au nanoparticles, the scattering vector (q) value decreased to 0.15288 A^{-1} with the corresponding interparticle spacing increasing to 4.1 nm. This 1.3 nm increase in spacing due to polymer assembly of Thy−Au nanoparticles was found to be similar to the distance previously observed with monoblock polymer-assembled gold nanoparticles.[17] There is also additional evidence to our assembly formation hypothesis shown in Figure 1, where a polymer chain separates the nanoparticles in the assemblies.

The advantage of using controlled block length diblock copolymers is to probe the nanoparticle cluster distances by looking at the scattering from these assemblies at small angles (SAXS). The average center-to-center aggregate spacing was probed by using PS/S-triaz (13:13) and PS/S-triaz (27:13) block copolymers. Increasing the corona-forming unfunctionalized polystyrene part of the micelle from 13000 to 27000 would be expected to increase the distance between the aggregates. As predicted, the SAXS experiment confirmed the average aggregate spacing with an increase from 20 nm for PS/S-triaz (13:13) to 35 nm for PS/S-triaz (27:13) (Figure 5).

Effect of Nanoparticle/Diblock PS/S-triaz Copolymer Ratio. Diblock polymers can form several different morphologies depending on the relative incompatibility and the overall volume fraction of each block.[18] One of the most well-known ways to control morphology in a given diblock system is the addition of homopolymers that are compatible with one of the blocks.[19] These homopolymers can preferentially phase segregate to that block and swell its volume by causing a shift in morphology. In our assembly system, Thy−Au nanoparticles were only assembled with the triaz-functionalized block; in a similar way we can induce the morphological control by changing the ratio of diblock copolymer to nanoparticle. The assemblies formed by incubating PS/S-triaz (27:26) diblock copolymer with increasing amounts of Thy−Au nanoparticle are shown in Figure 6.

(16) (a) Ballauff, M. *Curr. Opin. Colloid Interface Sci.* **2001,** *6*, 132−139. (b) Reetz, M. T.; Winter, M.; Breinbauer, R.; Thurn-Albrecht, T.; Vogel, W. *Chem. Eur. J.* **2001,** *7*, 1084−1094.

(17) Martin, J. E.; Wilcoxon, J. P.; Odinek, J.; Provencio, P. *J. Phys. Chem. B* **2000**, *104*, 9475−9486.

(18) Tuzar, T.; Kratochvil, P. In *Surface and Colloid Science*; Matijevic, E., Ed.; Plenum Press: New York, 1993; Vol. 15, p 1.

(19) (a) Ouarti, N.; Viville, P.; Lazzaroni, R.; Minatti, E.; Schappacher, M.; Deffieux, A.; Borsali, R. *Langmuir* **2005,** *21*, 1180−1186. (b) Zhao, J. C.; Jiang, S. C.; Ji, X. G.; An, L. J.; Jiang, B. Z. *J. Polym. Sci., Part B: Polym. Phys.* **2004,** *42*, 3496−3504. (c) Zhang, L.; Eisenberg, A. *J. Am. Chem. Soc.* **1996**, *118*, 3168. (d) Zhang, L.; Eisenberg, A. *Science* **1995**, *268*, 1728.

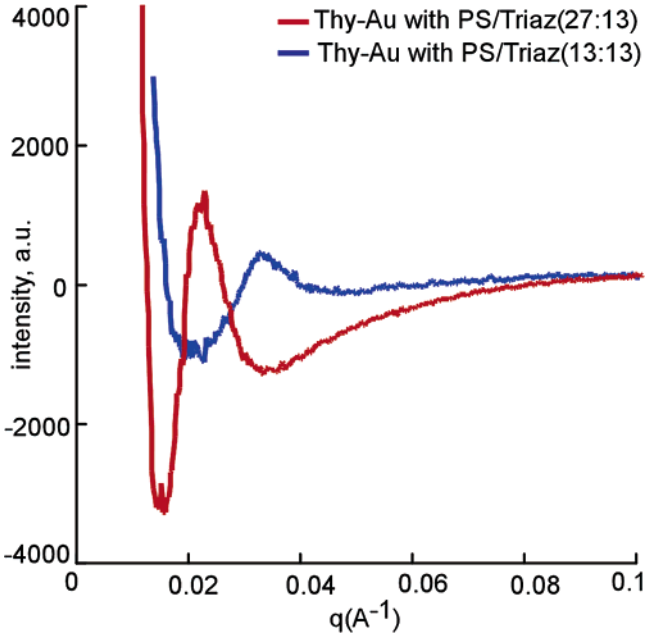

Figure 5. SAXS curves of structures formed by assembly of Thy−Au with PS/S-triaz (13:13) and PS/S-triaz (27:13) block copolymers which feature different polystyrene chain lengths (in the unfunctionalized blocks) give increases in interaggregate spacing.

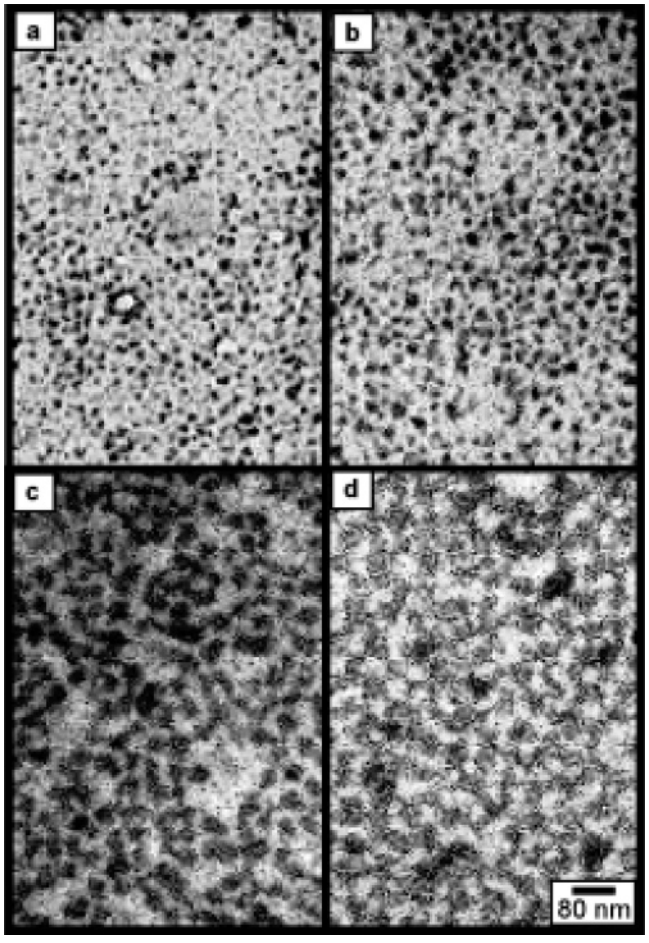

Figure 6. TEM images of the PS/S-triaz (27:26) diblock assembly as the Thy−Au weight ratio is increased from (a) 1/8, (b) 1/4, (c) 1/2, and (d) 1/1 (Thy−Au/diblock copolymer).

Spherical aggregate formation was evident from these micrographs even at relatively low polymer nanoparticle ratios (Figure 6a).

As more nanoparticle is incorporated into the polymer mortar, Thy−Au nanoparticles selectively swelled the functionalized block, causing a shift in morphology. These aggregates were expected to grow until the polymer was saturated with Thy−Au nanoparticle. At this saturation point, a transfer started to occur toward linked spheres, eventually ending with a structure similar to lamella morphology.

Conclusion

In conclusion, diblock copolymer assembly of gold nanoparticles provides an effective synthetic means to create discrete aggregates of nanoparticles with controlled size. The role of each of these blocks on the aggregate size was investigated by synthesizing two different series of diblock copolymers. Characterization using TEM, DLS, and SAXS revealed a distinct behavior pattern for each system. Our findings demonstrate that molecular recognition units attached to polymers can be used to create structures that are similar in solution and in the solid state, providing us efficient thermodynamical control of these stable assemblies. This "bricks and mortar" nanoparticle assembly strategy by using diblock copolymers will be further extended to electrically and magnetically active systems and will be reported in due course.

Experimental Section

Materials. All chemicals were reagent grade, purchased from Aldrich or Merck, and were used as received. Monomers (styrene and 4-chloromethylstyrene) were purified from the inhibitor using a short alumina plug.

Synthesis. Thy−Au nanoparticles (2 nm core diameter) were synthesized using our previously published procedures.[20]

PS/S-CMS polymers were synthesized via nitroxide-mediated controlled radical polymerization. The polystyrene (PS) block was created first, purified by precipitation in methanol from remaining monomer, and then polymerization of the styrene and 4-chloromethylstyrene (S/CMS) mixture to yield the functionalizable block took place.

Polymer Functionalization. These polymers were then converted into the diaminotriazine-functionalized polymers (PS/S-triaz) through reaction with sodium cyanide followed by dicyandiimide.[11] Complete conversion (within NMR detection limits) was determined using the side-chain CH_2 group resonance.

Characterization. Number-averaged molecular weights (M_n) and polydispersity indices (PDI) of the polymers in THF solutions were determined from gel permeation chromatograms (GPC) acquired on an in-house built GPC system using PL Caliber data collection software, three-column set (Polymer Labs, Inc.; PLgel 5 μm columns, 300 × 7.5 mm, 10^3, 10^4, and 10^5 Å pore size), with an RI detector (Waters 403). The system was calibrated with respect to polystyrene standards (Polymer Labs, Inc.). CMS content was calculated according to ^{1}H NMR peak integration (using a Bruker AC-200 spectrometer operating at 200.13 MHz for ^{1}H) to an estimated error of ±5% CMS content. NMR spectra were taken in $CDCl_3$.

Small-Angle X-ray Scattering (SAXS). To avoid kinetic entrapment by solvent evaporation effects, solid polymer samples (ca. 10 mg) in the precipitated powder form were annealed at 150

(20) Boal, A. K.; Gray, M.; Ilhan, F.; Clavier, G. M.; Kapitzky, L.; Rotello, V. M. *Tetrahedron* **2002,** *58*, 765−770.

°C under vacuum for 2 days and quenched to room temperature. Cu Kα X-rays (1.54 Å) were generated in an Osmic MaxFlux source with a confocal multilayer optic (OSMIC, Inc.). Images were taken with a Molecular Metrology, Inc., camera consisting of a three pinhole collimation system, 150 cm sample-to-detector distance (calibrated using silver behenate), and a two-dimensional, multiwire proportional detector (Molecular Metrology, Inc.). The entire X-ray path length was evacuated from the optic to the detector to reduce the background from air scattering. This setup allowed neglect of the correction for background scattering as proved by experiment. Two-dimensional images were reduced to the one-dimensional form using angular integration. Scattering vectors (q) were calculated from the scattering angles (θ) using $q = 4\pi \sin \theta/\lambda$, and particle spacings (D) were calculated from Gaussian fits to the principal scattering maxima of the Lorentz-corrected intensities using $D = 2\pi/q$.

Acknowledgment. This research was supported by NSF [CHE-0518487] and the University of Massachusetts Center for Hierarchical Manufacturing (NSEC, DMI- 0531171)

CM0614968